J Mater Sci (2010) 45:5318–5322
DOI 10.1007/s10853-010-4577-2

An X-ray absorption approach to mixed and metallicity-sorted single-walled carbon nanotubes

Paola Ayala · Hidetsugu Shiozawa · Katrien De Blauwe · Yasumitsu Miyata · Rolf Follath · Hiromichi Kataura · Thomas Pichler

Received: 16 April 2010 / Accepted: 28 April 2010 / Published online: 11 May 2010

Abstract Carbon based structures have been widely studied by X-ray absorption (XAS), also called NEXAFS, which is a very useful bulk probing method that allows examining the unoccupied density of states (DOS) and the site selective bonding environment. Two very well known spectral features in the XAS core level spectrum are the σ^* and π^* bands, and both have been analyzed in several studies for graphitic-like systems. However, among all the carbon materials, the unique one-dimensional electronic properties attributed to single-walled carbon nanotubes (SWCNTs) exhibit features that reveal clearly their electronic structure in the core level XAS spectrum. In this article, we outline the C1*s* response in XAS, which is related to the DOS of the conduction band in SWCNTs and its fine structure, revealed by experiments performed on metallicity-sorted SWCNT material. The progress in the identification of changes in the site selective conduction band electronic structure with XAS is discussed in detail.

P. Ayala (✉) · K. De Blauwe · T. Pichler
Faculty of Physics, University of Vienna, Strudlhofgasse 4, 1090 Vienna, Austria
e-mail: paola.ayala@univie.ac.at

H. Shiozawa
Advanced Technology Institute, University of Surrey, Guildford GU2 7XH, UK

Y. Miyata
Department of Chemistry, University of Nagoya, Nagoya 464-8602, Japan

R. Follath
BESSY II, 12489 Berlin, Germany

H. Kataura
Nanotechnology Research Institute, National Institute of Advanced Industrial Science and Technology, Tsukuba 305-8562, Japan

H. Kataura
JST, CREST, Kawaguchi, Saitama 330-0012, Japan

Introduction

Single-walled carbon nanotubes (SWCNTs) are one-dimensional (1D) crystalline structures with peculiar electronic properties. The carbon atoms constituting the backbone of the tubular structure form σ bonds with their neighbors, leaving one electron in a π orbital which is responsible for the intriguing electronic structure of these materials. Furthermore, to understand the studies here presented it is useful to keep in mind that the geometric structure of a SWCNT renders its metallic or semiconducting nature.

Commonly used nanotube synthesis techniques are nowadays able to produce gram quantities of SWCNTs but they are not metallicity-sorted as-grown. Positive developments have been made in controlling and optimizing the synthesis, as well as the purification and separation of nanotubes by metallicity and chirality. Taking advantage of this, we have made use of purely metallic and purely semiconducting samples produced by density gradient ultracentrifugation (DGU) [1]. Techniques such as scanning tunneling microscopy, photoemission spectroscopy, nuclear magnetic resonance, optical absorption, among others, have been able to identify the characteristic features of the electronic structure of SWCNTs. Combining XAS as a bulk probing technique with the availability of metallicity-sorted material, we show here that it is possible to study the long theoretically predicted electronic structure of SWCNTs on a buckypaper (see left side inset in Fig. 1).

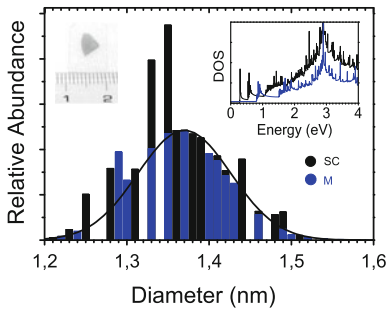

Fig. 1 The nanotube material probed for these studies are bundles with a Gaussian diameter distribution centered at 1.37 nm and a spread of ±0.08 nm. The histogram shows the relative abundance of semiconducting (*black*) and metallic (*blue*) species. The corresponding diameter cumulative tight binding calculation of the DOS for metallic and semiconducting SWCNTs is shown in the right side inset. Additionally, the nanotube material probed was in the form of a buckpaper such as the picture displayed as inset in the top left corner (Color figure online)

Focusing deeper on the technique, it is worth recalling that XAS is a powerful tool revealing the features in the unoccupied density of states (DOS). It has been widely used to study materials made of carbon atoms in its three possible hybridizations. For instance, the electronic structure of graphite has been widely studied experimentally and theoretically and the σ^* and π^* thresholds have been examined by various authors [2–5]. An intense debate existed around a discrepancy of the position of a peak appearing 3 eV above the Fermi level (E_F) in the ground state DOS, whereas experimental XAS observations found that peak dislocated 1 eV. This peak is associated to the π^* resonance and its dislocation has been found to be strongly affected by excitonic effects. Also, the σ^* is strongly influenced by excitonic effects but we will not focus on it in this contribution.

The purpose of this article is assessing the electronic states is SWCNTs using XAS. More specifically, we focus on the nature of the π^* resonance and the fine structure that we have observed in this feature. Along this manuscript, we describe how this can be associated to the van Hove singularities (vHs) characteristically observed in the DOS of SWCNTs.

Experimental

Samples

The studies described in this contribution have been made on films of purified SWCNT with a characteristic narrow Gaussian diameter distribution centered at 1.37 nm and a spread of ±0.08 nm as depicted in Fig. 1. Both, arc discharge and laser ablation pristine SWCNTs have been used. In addition, arc discharge samples, later separated according to metallicity via DGU [1], have been employed. A subsequent filtration has been used, which allows the formation of mats of so-called buckypaper of purely metallic and purely semiconducting SWCNTs (see example of the metallic buckypaper on the top left side of Fig. 1). This facilitates the use of samples as a bulk sample which can later easily be mounted on a conducting sample holder [6].

The quality of these samples is checked by photoemission studies, which reveal an overall purity of better than 99% regarding the catalysts other carbon impurities, due to the absence of any other photoemission signals beyond the carbon response from the separated SWCNT. The signal of the metal particles was below the detection limit of 0.5% of the carbon C1*s* signal, showing the high purity of the samples [7]. The same holds for the purity of the samples regarding the details in the valence and conduction band response of the SWCNT. Previous results on the purity of metallicity integrated samples [8–10] showed a direct correlation between the purity of the samples and the observation of the 1D van Hove singularities in the valence band photoemission response. This is important because any remaining impurity beyond 1% yields to impurity scattering which broadens the overall 1D photoemission response of the SWCNT [9, 11].

XAS experiments

All the measurements are performed on a film of SWCNTs annealed above 800 K in ultra-high vacuum. XAS experiments here reported were performed at the beamline UE52PGM at Bessy II. XAS spectra were recorded in partial yield and drain current modes. All the the NEXAFS experiments here reported were performed at the beamline UE52PGM at Bessy II, which has a resolving power ($E/\Delta E$) of $4 \cdot 10^4$.

Results and discussion

As mentioned in the introductory section, studying the C1*s* response in XAS is a very useful way to prove the conduction band of the system. This feature has been analyzed for various carbonaceous materials along the years. However, let us focus merely on graphite and carbon nanotubes. The overall XAS absorption spectral patterns in the C1 response are depicted in Fig. 2. The lines depicted from bottom to top are high-resolution XAS spectra recorded on the C1*s* edge of highly oriented pyrolitic graphite, as-grown bundles of SWCNTs with random metallicity and sorted semiconducting and metallic species. The spectra corresponding HOPG and metallicity-mixed samples has been reproduced from Ref. [12].

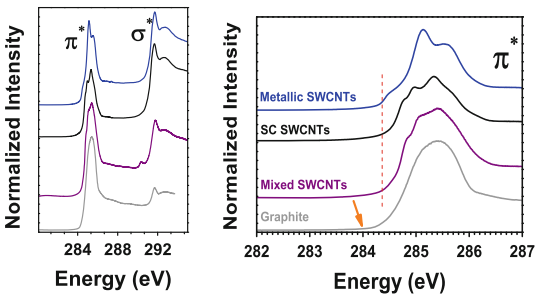

Fig. 2 *Left panel*: the lines depicted from bottom to top are high-resolution XAS spectra recorded on the C1*s* edge of graphite, as-grown bundles of SWCNTs with random metallicity and sorted semiconducting and metallic species. *Right panel*: close up into the C1*s* π^* absorption edge of the same types of samples

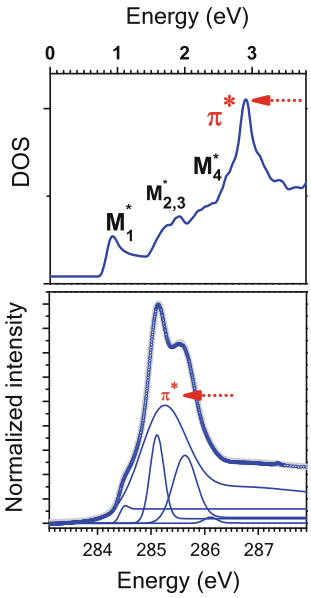

Fig. 3 Close up of the high-resolution XAS C1*s* π^* absorbtion edges (*circles*) of metallic SWCNTs together with the results of a line shape analysis (*lines*). The *top panel* depicts the diameter cumulative TB DOS broadened by the experimental resolution. This calculation takes into account bundles of SWCNTs with a Gaussian diameter distribution centered at 1.37 nm and a spread of ±0.08 nm The lables denote the vHs ($M^*_{1...4}$), and the overall conduction band (π^*)

The overall shape in all these cases exhibits the well known π^* resonance at 285.4 eV and the σ^* threshold at 291.7 eV [13], which has also been reported with core level EELS on the C1*s* edge of SWCNTs [10] and previous XAS results on SWCNTs [14–16]. This is the first hint that the signature of the conduction band in the metallicity separated SWCNTs must include a reminiscent shape related to the graphite response, which is indeed the case. However, examining closer the XAS C1*s* response of the SWCNTs as shown in Fig. 2, a fine structure appears on the π^* resonance. It had been suggested that the pronounced features appearing on the π^* peak could be related to the distinct vHs in the unoccupied DOS of the SWCNTs [12, 17]. The clearly resolved fine structure features in the XAS spectra of bulk metallicity-mixed SWCNTs address the concomitant response of metallicity-sorted SWCNTs. However, only the use of SWCNTs which are metallicity-sorted truly discerns unambiguously the fine structure that fingerprints the 1D response of metallic and semiconducting species.

Let us now analyze separately the 1D DOS in the conduction band of sorted metallic and semiconducting SWCNTs, looking at the high-resolution C1*s* edge XAS spectra depicted both in Figs. 3 and 4, respectively. The π^* response of the metallic and semiconducting species exhibits a unique fine structure. In both cases, in order to disentangle the independent fine structures we made a fine lineshape analysis. For this, we have taken into account the position of the vHs obtained from the diameter cumulative tight binding (TB) calculations corresponding to the two different types of samples (shown in Fig. 1). As depicted in the upper pannels of Figs. 3 and 4, we have applied a Gaussian broadening to the DOS calculated for the conduction bands correspondingly, to better compare the theory with the XAS experiments.

First, the metallic SWCNTs samples exhibit the π^* resonance fine structure depicted in Fig. 3. To unravel this fine structure, we performed a line shape analysis using Gaussian components. As it is clearly seen, the solid lines used in this deconvolution correspond to the vHs and a broad Voigtian for the π^* peak which is related to the graphite lineshape, as indicated in the figure. The π^* peak is observed at 285.26 eV in the case of the purely metallic samples. The additional foot at the low-binding energy was fitted using a cumulative Gaussian folded by a Fermi function. In addition, the fine structure corresponding to the metallic sample response, exhibits peaks positioned at 285.10, 285.65 eV and a shoulder at 286.1 eV. An additional foot in the case of metallic SWCNTs is located at 284.5 eV. This can be attributed to the onset of the constant 1D DOS at the E_F in the case of the metallic nature of the probed sample. Analyzing now the features of the fine structure observed in the π^* response corresponding to the purely semiconducting type of samples, again a broad Voigtian has been used to identify the π^* graphite reminiscent, which is centered at 285.3 eV and it is in particularly good agreement with the values reported for graphite. The semiconducting fine structure is observed as peaks at 284.75, 284.95, 285.35 eV and as shoulders at 285.7 and 286.05 eV.

The comparison of the detailed line shape analysis to the broadened metallicity selected diameter cumulative DOS is shown in the upper panels of Figs. 3 and 4. The scaled calculation can be positioned according to the C1*s* binding energy, which can be in turn directly associated to

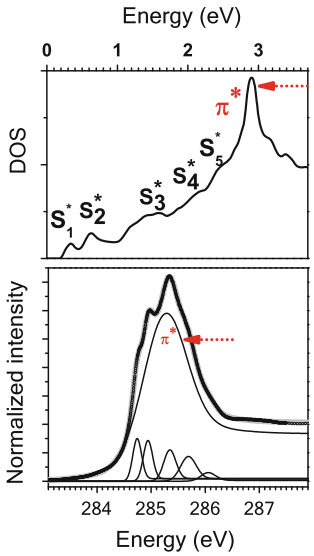

Fig. 4 Close up of the high-resolution XAS C1*s* π^* absorbtion edges (*circles*) of semiconducting SWCNTs together with the results of a line shape analysis (*lines*). The *top panel* depicts the diameter cumulative TB DOS broadened by the experimental resolution. This calculation takes into account bundles of SWCNTs with a Gaussian diameter distribution centered at 1.37 nm and a spread of ±0.08 nm. The labels denote the vHs ($S^*_{1...5}$), and the overall conduction band (π^*)

respective XAS onsets. It is worth noting that in analogy to photoemission studies [7], the same fine structures (S^*_1 to S^*_5 and M^*_1 to M^*_4) are observed in high-resolution XAS. With this, the actual positions and widths of the diameter cumulative vHs peaks are in very good agreement with the TB calculations without any further scaling, while the broad π^* resonance, which is well known to be strongly affected by the C1*s* core hole, is dislocated as marked by the red arrows in both Figs. 3 and 4.

Previous studies on SWCNTs samples with mixed metallicity, reported the π^* peak related to the DOS at the M point of the underlying graphene structure downshifted by about 2 eV due to the C1*s* core hole effects [3, 12, 18]. This confirmed in turn its strongly excitonic nature. On the other hand, it is worth noting that in molecules like C_{60} [19] and $C_{59}N$ [20] the bands are associated to the molecular orbitals and the core hole effects are much less pronounced.

In the π^* peaks we have resolved experimentally, it is clear that this line is strongly excitonic and downshifted by core hole effects. Nevertheless, we show that TB calculations allow directly identifying the individual fine structures in the unoccupied DOS straightforwardly. The core hole effect in the broad C1*s* π^* resonance resembles bulk sp^2 carbon, whereas the small core hole effects in the resonances due to vHs are attributed to molecular excitations.

These results substantiate the intriguing composition of bulk and molecular features in the electronic excitation spectrum of SWCNTs. Revealing the composed C1*s* response along the SWCNTs axis and the circumferential direction justify to certain extent the ever found difficulties to correctly describe the details in the C1*s* response of this 1D solids in theory so far. The diameter cumulative TB calculations used here allow us to apply an identification starting point for the whole set of chiralities in the diameter range given by the sample characteristics.

Conclusions

One of the major gains of this XAS result is that it completes our knowledge on the 1D electronic structure of SWCNTs on the bulk scale by directly accessing the details in the conduction band. This represents a model or base to compare molecular like conduction band DOS of the vHs in polarization perpendicular to the tube axis, such as in the well studied case of other molecular systems like functionalized fullerenes [20]. This sets the basis for analyzing the electronic structure and bonding environment in functionalized, metallicity selected carbon nanotubes with unprecedented detail.

Acknowledgements This work was supported by the Austrian Science Fund through project FWF P21333-N20 and the German Research Foundation through project DFG PI 440-4/5. H.S. acknowledges the Leverhulme Trust and the EPSRC through a Portfolio Partnership grant. We acknowledge the technical assistance from S. Leger, R. Hübel, and R. Schönfelder from the IFW-Dresden, as well the fruitful discussions and collaboration with K. Kramberger, M. Knupfer, J. Fink, X. Liu, H. Kuzmany, A. Grüneis, and F. Simon. We acknowledge the Helmholtz-Zentrum Berlin—Electron storage ring BESSY II for provision of synchrotron radiation at beamline UE52PGM. The research leading to these results has received funding from the European Community's Seventh Framework Programme (FP7/2007-2013) under grant agreement n.°226716.

References

1. Arnold MS, Green AA, Hulvat JF, Stupp SI, Hersam MC (2006) Nat Nanotechnol 1:60
2. Ahuja R, Bruhwiler PA, Wills JM, Johansson B, Martensson N, Eriksson O (1996) Phys Rev B 54:14396
3. Bruhwiler PA, Kuiper P, Eriksson O, Ahuja R, Svensson S (1996) Phys Rev Lett 76:1761
4. Weng X., Rez P., Ma H. (1989) Phys Rev B 40:4175
5. Vedrinskii RV, Kraizman VL, Novakovich AA, Machavariani GY, Machavariani VS (1994) J Phys Condens Matter 6:11,045
6. Miyata Y, Yanagi K, Maniwa Y, Kataura H (2008) J Phys Chem C 112:13,187
7. Ayala P, De Blauwe K, Shiozawa H, Feng Y, Kramberger C, Silva S, Follath R, Kataura H, Pichler T (2009) Phys Rev B 80:205427
8. Ishii H, Kataura H, Shiozawa H, Yoshioka H, Otsubo H, Takayama Y, Miyahara T, Suzuki S, Achiba Y, Nakatake M,

Narimura T, Higashiguchi M, Shimada K, Namatame H, Taniguchi M (2003) Nature 426:540
9. Rauf H, Pichler T, Knupfer M, Fink J, Kataura H (2004) Phys Rev Lett 93:096805
10. Pichler T (2001) New Diam Front Carb Tech 11:375
11. Shiozawa H, Ishii H, Kihara H, Sasaki N, Nakamura S, Yoshida T, Takayama Y, Miyahara T, Suzuki S, Achiba Y, Kodama T, Higashiguchi M, Chi XY, Nakatake M, Shimada K, Namatame H, Taniguchi M, Kataura H (2006) Phys Rev B 73:075406
12. Kramberger C, Rauf H, Shiozawa H, Knupfer M, Buchner B, Pichler T, Batchelor D, Kataura H (2007) Phys Rev B. 75:235437
13. Mele EJ, Ritsko JJ (1979) Phys Rev Lett 43:68
14. Goldoni A, Larciprete R, Petaccia L, Lizzit S (2003) J Am Chem Soc 125(37): 11,329
15. Larciprete R, Goldoni A, Lizzit S, Petaccia L (2005) Appl Surf Sci 248(1-4):8
16. Nikitin A, Ogasawara H, Mann D, Denecke R, Zhang Z, Dai H, Cho K, Nilsson A (2005) Phys Rev Lett 95(22):225,507
17. Shiozawa H, Pichler T, Kramberger C, Rummeli M, Batchelor D, Liu Z, Suenaga K, Kataura H, Silva SRP (2009) Phys Rev Lett 102:046804
18. Shirley EL (1998) Phys Rev Lett 80(4):794
19. Goldoni A, Cepek C, Larciprete R, Sangaletti L, Pagliara S, Paolucci G, Sancrotti M (2002) Phys Rev Lett 88(19):196,102
20. Pichler T, Knupfer M, Golden MS, Haffner S, Friedlein R, Fink J, Andreoni W, Curioni Keshavarz-K M, Bellavia-Lund C, Sastre A, Hummelen J, Wudl FA (1997) Phys Rev Lett 78(22):4249